ASEG-PESA 2015
Geophysics and Geology together for Discovery
24th International Geophysical Conference and Exhibition
15–18 February 2015 Perth, Western Australia

Passive seismic imaging without velocity model prior to imaging

Mohammad Javad Khoshnavaz
Deep Exploration Technologies Centre (DETCRC), Department of Exploration Geophysics at Curtin University
mj.khoshnavaz@postgrad.curtin.edu.au

Andrej Bóna
Deep Exploration Technologies Centre (DETCRC), Department of Exploration Geophysics at Curtin University
a.bona@curtin.edu.au

Milovan Urosevic
Deep Exploration Technologies Centre (DETCRC), Department of Exploration Geophysics at Curtin University
m.urosevic@curtin.edu.au

SUMMARY

There are two types of passive seismic monitoring: down-hole and surface monitoring. In this paper, we introduce a new surface monitoring technique that does not require trigger time and any seismic velocity information prior to imaging. Therefore, this technique can be considered as a velocity independent monitoring technique. We have calculated the radius ot the curvature of the propagated wave-front from the passive source to the receivers deployed on the surface. The passive source coordinates are expressed in terms of the curvature. Computational experiments with synthetic data examples confirm the theoretical expectations and demonstrate the practical feasibility of the proposed technique.

Key words: Passive seismic, velocity independent, curvature of wave front.

INTRODUCTION

Passive seismic imaging is the study of seismic wave propagation through the Earth without the use of a dedicated controlled seismic source. Seismic signals generated from fault displacement in earthquakes, drilling and hydraulic fracturing during high-pressure fluid injection into boreholes, are typically known as passive seismic signals. Passive-seismic imaging techniques have different uses, from targeting ore deposits in mining industry to finding natural resources in oil/gas industry by micro-seismic monitoring.

Passive seismic imaging has applications in both mining and oil industry. Some of its applications in mining industry are related to: control of seismicity, management of seismic hazards in mines and to seismic-while-drilling methods (Sun et al. 2014). Localisation of micro earthquakes caused by high pressure fluid injection into a geological formation with low permeability has an important role in oil/gas industry.

According to Maxwell et al. (2010), two main methods of passive seismic localisation are used in industry: down-hole and surface localisation. A limited number of 3C receivers (8-40) are used for down-hole localisation. They are normally deployed into one or more observation wells near the passive source to increase signal-to-noise (S/N) ratio (Eisner et al., 2011). The considerable advantage of down-hole monitoring technique regards to its high S/N. On the other hand, down-hole monitoring is quite expensive because of drilling, logging and using 3C down-hole receivers. In addition, the observation well cannot be used for production during recording (Chambers et al., 2008). Finally, the technique is also not able to prepare sufficient aperture and fold for algorithms based on spatial covering (Duncan and Eisner, 2010). Surface localization is an alternative technique to locate passive sources in the subsurface. Duncan and Eisner (2010) list different algorithms that have been developed within the last few decades in surface passive seismic imaging: applying reverse-time migration and wave-form extrapolation to detect the earthquake centres was proposed and successfully tested by McMechan (1982), McMechan et al. (1985). Passive seismic emission tomography, which is a semblance-based detecting technique, introduced and successfully applied to identify hydrothermal fields in Iceland by Kiselevitch et al. (1991). The application of this method on surface micro-seismic localization is reported by Duncan (2005) and Lakings et al. (2006).

In this article, we introduce another approach for surface passive seismic localization. Using this approach, there is no need to have any velocity model prior to imaging. It uses the local derivatives of travel time with respect to offset. We assume that seismic wave propagates through an effective homogeneous medium. This assumption is correct for many geological lithologies, including vertical inhomogeneity. First, we explain and illustrate the imaging technique with different synthetic examples. Finally, we discuss about the future of the research on surface passive seismic localization.

METHOD

In this part, we explain the concept of the curvature (R) of emitted wave-front and our velocity independent surface passive seismic localization algorithm.

Consider a fixed source (S) in an effective homogeneous medium with the coordinates of (x_s, z_s) from an arbitrary benchmark on the surface named O (Figure 1). In the case of wave emission through an effective constant velocity medium (v), the effective slowness (p) is defined as the reverse proportion of the velocity (v).

$$p = \frac{1}{v} \tag{1}$$

We derived the curvature in terms of horizontal slowness (p_1), apparent curvature (p_2) and the effective slowness (p), as given by the following equation.

$$R = \frac{p}{p_2}\left(1 - \frac{{p_1}^2}{p^2}\right) \quad (2)$$

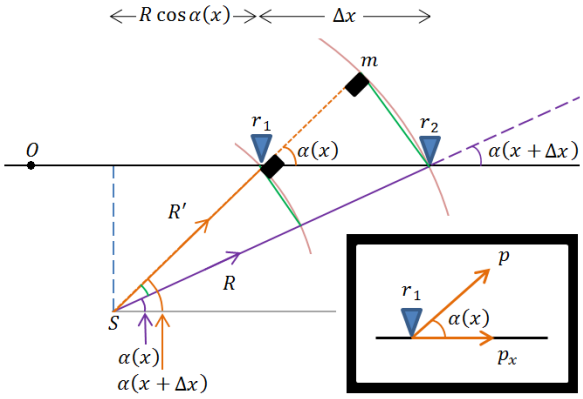

Figure 1. Geometry of the reflected wavefront from the image source (*S*).

Based on the geometry of the emitted wave-front shown in Figure 1, the spatial coordinates of the image source (x_s, z_s) are expressed by

$$x_s = x - R\cos(\alpha) \quad (3)$$

$$z_s = R\sin(\alpha) \quad (4)$$

where α is the angle between the observation line on surface $(z = 0)$ and the direction of the emitted ray reaching to the receiver and x is the coordinate of the receivers on the surface (Figure 1). The trigonometric ratios are in terms of local slope and effective slowness. Differentiation of either of Equations 3 and 4, using the calculated curvature, doing some algebra and simplification give the following velocity function, which is in terms of the local derivatives of time with respect to offset.

$$p^2 = {p_1}^2 - \frac{3p_1{p_2}^2}{p_3} \quad (5)$$

p_3 denotes the third derivative of time with respect to offset. As can be seen, the expressed velocity formula (Equation 5) is independent from travel time and offset. That is why the calculated velocity can be useful for passive seismic monitoring and earthquake seismology, when the trigger time and the coordinates of the seismic source are unknown.

To summarise the localization technique, first, we should calculate the local derivatives of time with respect to offset to estimate the velocity and the curvature of emitted wave-form. Substitution of these measurements in Equations 3 and 4 gives the spatial coordinates of the passive source.

EXAMPLES

In the first example, we use a 2D synthetic record generated for a source fixed in a homogenous space with the P-velocity of 2500 m/s (Figure 2a). The horizontal and vertical coordinates of passive source are 700 m and 500 m, respectively. Ricker wavelet with the dominant frequency of 20 Hz has been used to generate the data. We also set 2 millisecond and 20 meter for sampling interval and receiver spacing, respectively. Figure 2b shows the modelled passive record.

a)

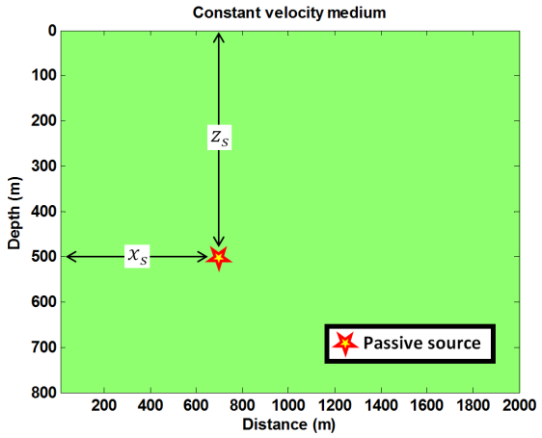

b)

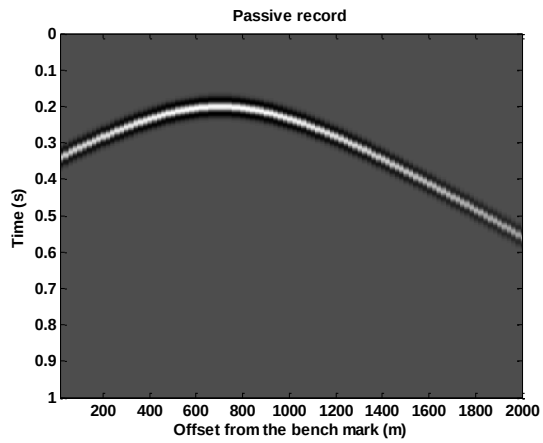

Figure 2. a) Passive seismic model for a source fixed in a homogenous space b) passive record before adding noise.

To show the independence of the imaging technique from actual travel time used to generate the passive record, we shifted the passive event in time by 0.3 s. After that, we added random noise onto the generated record so that the S/N is 2 (Figure 3). We considered 10 geophones in each station on the surface to stack the records. The stack section is illustrated in Figure (4). As we discussed in the previous part, having multi channels and stacking are defined as privileges of surface passive seismic localization techniques over down-hole methods.

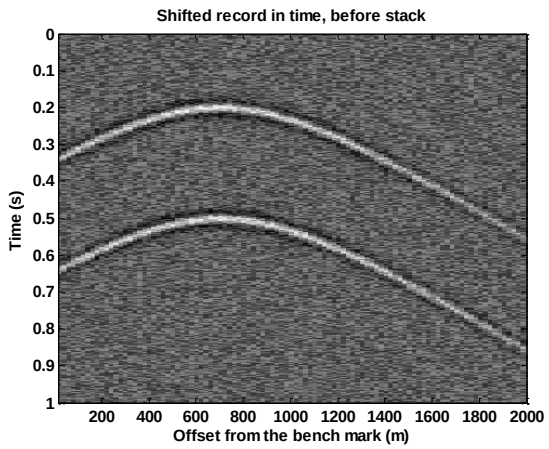

Figure 3. Shifted passive record generated in time by 0.3 *s* with the S/N of 2.

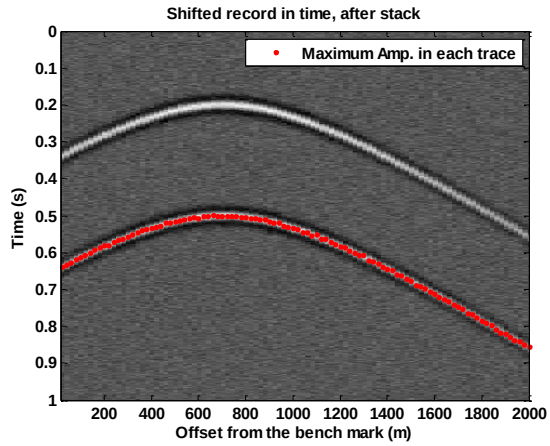

Figure 4. Maximum amplitudes are picked after stacking.

In the next step, we picked maximum amplitudes along each trace, within the window of the detected event (Figure 4). We can use local fitting of a polynomial/hyperbolic curve to the data to take advantage of the local nature of the method. Using least square technique one hyperbola is fitted onto the maximum amplitudes. Least square fitting gives the relevant coefficients for the polynomial/hyperbolic fitting. Substituting these coefficients in the polynomial/hyperbolic equation, one can easily differentiate the equation with respect to offset to calculate p_1, p_2 and p_3 in each point.

Using the calculated derivatives, we directly estimated the velocity and the curvature of emitted waveform followed by the spatial coordinates of the passive source. The result of the passive monitoring algorithm for the passive source fixed in a homogenous space are listed in Table (1). As can be seen, the source is very well localized with the uncertainty of less than 0.5 percent.

	Velocity (m/s)	X-Coordinate (m)	Z-Coordinate (m)
Expected	2500	700	500
Estimated	2495	701	498

Table 1. Expected and estimated results for the passive record shown in Figure 3.

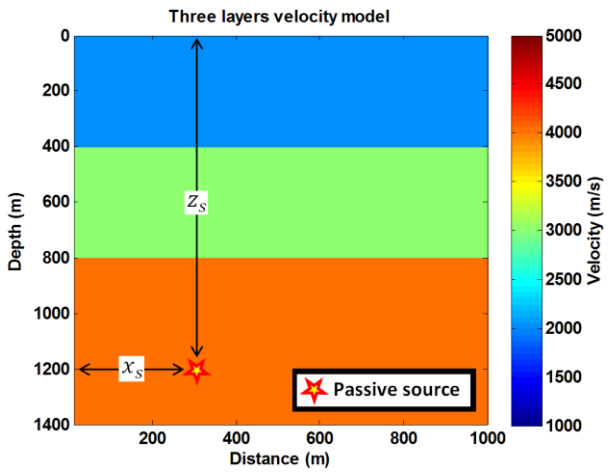

Figure 5. Three horizontal layered velocity model

In the next example, we test the algorithm on a velocity model that contains three horizontal formations (Figure 5). This model is suitable for many sedimentary structures. We used the compressional velocity of 2000, 3000 and 4000 m/s for the first, second and the third layer of the model, from top to bottom. We also set 400 m as the thickness of the first and the second layer. The source is fixed in x_s=300 m and z_s=1200 m. Ricker wavelet with the dominant frequency of 20 Hz has been used to generate the data. 1 millisecond and 10 meters are chosen for sampling interval and receiver spacing.

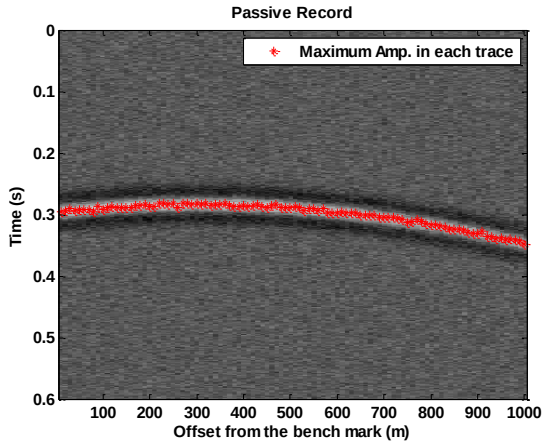

Figure 6. Shifted passive seismic record in time (0.15 ms) with the S/N of 2 for the velocity model shown in Figure 5 b) Maximum amplitudes are picked after stacking.

In this example, again, we shifted the passive record in time (0.15 s) that is generated by true travel time calculation. We also added Gaussian noise to the record so that the S/N is 2. 8 receivers are set in each station on the observation line on the surface to stack the records. The stack section obtained from the 10 passive records is shown in Figure (6). Table (2) indicates the expected and estimated velocity and the passive source coordinates. The passive source is fairly imaged with less than 0.5 percent of error. The error belongs to least square fitting and the noise.

	Velocity (m/s)	X-Coordinate (m)	Z-Coordinate (m)
Expected	2882	300	1200
Estimated	2879	301.2	1206

Table 2. Expected and estimated results for the passive record shown in Figure 5.

CONCLUSIONS

Local derivatives of travel time with respect to the location of geophones on surface carry useful information about velocity and passive source location in the subsurface. We have used the derivatives and have designed a velocity-less surface passive seismic monitoring algorithm to locate sources fixed in homogeneous and vertical inhomogeneous media. The main advantage of the proposed technique is that it does not need a velocity model prior to imaging. Furthermore, this method maps the passive source coordinates directly without ray-tracing and tomography followed by inversion.

The monitoring technique was applied on 2D examples. Using another observation line on the surface, the method is extendable to 3D case. In the presented article, we used P-velocity to locate the passive source but the technique is also capable to locate the source by S-velocity. One can extend the proposed technique to locate passive sources fixed in an arbitrary layered model in future. In order to do that, 3D arrays

and both P- and S- wave velocities should be used to decrease uncertainties. If we can estimate the derivatives locally (e.g. by fitting polynomial curves to only a small part of travel time curve), we could extend the method to an anisotropic media; the method would estimate different velocities for different angles. The accuracy of such application needs to be tested as the method relies on spherical (locally) wavefronts.

ACKNOWLEDGMENTS

The work has been supported by the Deep Exploration Technologies Cooperative Research Centre whose activities are funded by the Australian Government's Cooperative Research Centre Program. This is DETCRC document 2014/546.

REFERENCES

Duncan, P. M., 2005, Is there a future for passive seismic? : First Break, 23, 111–115.

Duncan, P. M., and Eisner, L.,2010, Reservoir characterization using surface microseismic monitoring: Geophysics, 75, 75A139–75A146. DOI: 10.1190/1.3467760

Eisner, L., De La Pena, A., Wessels, S., Barker, W., and Heigl, W., 2011, Why surface monitoring of microseismic events works, Third Passive Workshop, EAGE,.

Kochnev, I. V., Polyakov, V. S., Murtayev, I., Savin , V. G., Zommer, B. K., and Bryksin, I.V., 2007, Imaging hydraulic fracture zones from surface passive microseismic data: First Break, 25, 77–80.

Lakings, J. D., Duncan, P.M., Neale, C., and Theiner, T., 2006, Surface based microseismic monitoring of a hydraulic fracture well stimulation in the Barnett Shale: 76th Annual International Meeting, SEG, Expanded Abstracts, 605–608.

Maxwell, S., Rutledge, J., Jones, R., and Fehler, M., 2010, Petroleum reservoir characterization using downhole microseismic monitoring: Geophysics, 75, 75A129–75A137. DOI: 10.1190/?1.3477966

McMechan, G. A., 1982, Determination of source parameters by wavefield extrapolation: Geophysical Journal of the Royal Astronomical Society, 71, 613–628.

McMechan, G. A., Luetgert, J. H., and Mooney, W. D., 1985, Imaging of earthquake sources in Long Valley caldera, California, 1983: Bulletin of the Seismological Society of America, 75, 1005–1020.

Sun, B., Bóna, A., King, A., and Zhou, J., 2014, Diamond Drill-bit Seismic-While-Drilling Velocity Analysis Using Semblance and MUSIC from Hillside, South Australia: 76th Conference and Exhibition, EAGE, Expanded Abstracts, DOI: 10.3997/2214-4609.20140918.